Separation Science and Technology

Publication details, including instructions for authors and subscription information:
http://www.informaworld.com/smpp/title~content=t713708471

Studies of the Separation of Hydrogen Isotopes by a Pressure Swing Adsorption Process

Y. W. Wong[a]; F. B. Hill[a]; Y. N. I. Chan[ab]
[a] Department of Energy and Environment, Brookhaven National Laboratory Upton, New York [b] Shell Canada Ltd., Ontario, Canada

To cite this Article Wong, Y. W. , Hill, F. B. and Chan, Y. N. I.(1980) 'Studies of the Separation of Hydrogen Isotopes by a Pressure Swing Adsorption Process', Separation Science and Technology, 15: 3, 423 — 455

To link to this Article: DOI: 10.1080/01496398008068491

URL: http://dx.doi.org/10.1080/01496398008068491

SEPARATION SCIENCE AND TECHNOLOGY, 15(3), pp. 423-455, 1980

STUDIES OF THE SEPARATION OF HYDROGEN ISOTOPES BY A PRESSURE SWING ADSORPTION PROCESS

Y. W. Wong, F. B. Hill, and Y. N. I. Chan*
Department of Energy and Environment
Brookhaven National Laboratory
Upton, New York 11973

ABSTRACT

A theoretical and experimental study was made of the mechanism of the separation of a mixture of hydrogen isotopes by a two-column pressure swing adsorption process in which vanadium hydride was used as the solid phase. Theoretical predictions of process performance were compared with data from process experiments using hydrogen containing a trace of HT as feed. For process operation wholly within the monohydride phase, a postulated isotope effect in the rates of hydrogen absorption and desorption appeared to control process performance. When process operation involved transitions back and forth between the monohydride and dihydride phases, process performance was determined mainly by an equilibrium isotope effect.

INTRODUCTION

It has been recognized for many years that hydrogen isotopes can be separated by chromatographic techniques. Thus, as examples, Glueckauf and Kitt (1) achieved complete separation of gaseous deuterium and protium mixtures by using a displacement technique in a supported palladium column. Smith and Carter (2) tested the separation of tritium-protium mixtures using silica columns at liquid nitrogen temperatures and attained good reso-

---

*Present address: Shell Canada Ltd., Oakville, Ontario, Canada lution using elution chromatography. Even though large separation factors are obtained via techniques such as these, which are useful in separations for analytical purposes, these techniques when employed on a large scale have the disadvantages that they are not continuous and throughput with them is small.

In recent years, numerous techniques have been devised which permit continuous or semicontinuous operation of chromatographic separation processes which can be scaled up to throughputs of industrial interest. Such techniques include various forms of preparative chromatography (3), pressure swing adsorption (4,5), continuous countercurrent operation (6), cycling zone adsorption (7,8), and parametric pumping (9,10). Preparative chromatography techniques and pressure swing processes have been widely adopted industrially. Some of these processes and the very closely related process, parametric pumping, are capable of producing very large separation factors. Continuous countercurrent separations are also used industrially but require the use of moving beds.

In this study, attention is focused on the pressure swing process and its use in separating a tritium-protium mixture. Hamrin and Weaver (11) have attempted to use this process to separate deuterium and protium and obtained small deuterium enrichments. The palladium-hydrogen system was used in their study. This system exhibits a so-called normal isotope effect. That is, the solid phase affinity towards hydrogen isotopes increases in the order, tritium, deuterium, protium. Vanadium hydride was chosen for the present study because of its preferential uptake of a heavy isotope of hydrogen in the presence of a light isotope. It is thus preferred for the removal of a trace quantity of a heavy isotope from a mixture with a light isotope.

The equilibrium and kinetic properties of the vanadium-hydrogen-tritium system pertaining to isotope exchange have been measured by Reilly and Wiswall (12), Wiswall and Reilly (13), and Wong and Hill (14). The results of these investigations were used in the present study to guide the design and interpretation of pressure cycling experiments.

The present work was undertaken in order to obtain an understanding of the phenomena controlling the performance of the pressure swing process when carrying out the stated separation. To this end, an equilibrium theory of the operation of the pressure swing adsorption process as applied to the hydrogen isotope-vanadium hydride system is presented, experiments are reported on the separation of an $HT-H_2$ mixture, and theory and experiment are compared. Optimization of the process is not examined or discussed. A preliminary account of this work appears elsewhere (15).

PROCESS DESCRIPTION

The version of pressure swing adsorption examined here is the two-bed process known as heatless adsorption. As illustrated in Fig. 1, there are four steps during a complete cycle of operation. In the first step, a high pressure feed mixture is continuously supplied to Bed 1. During this step, sorbable components are taken up by Bed 1. At the same time, a portion of the purified effluent is taken off as high pressure product, and the remainder is throttled down to a lower pressure and directed to Bed 2 to purge previously sorbed species. In the second step, Bed 2 is pressurized with feed, and Bed 1 undergoes blowdown to the purge pressure. The third and fourth steps are the same as the first and second respectively except that the points of feed introduction and purge and blowdown removal are reversed with respect to Beds 1 and 2. The novelty of this process lies in the fact that, at least as a theoretical limit, with sufficient purified product used as purge, complete removal of the sorbable or preferentially sorbable components from the high pressure product can be achieved.

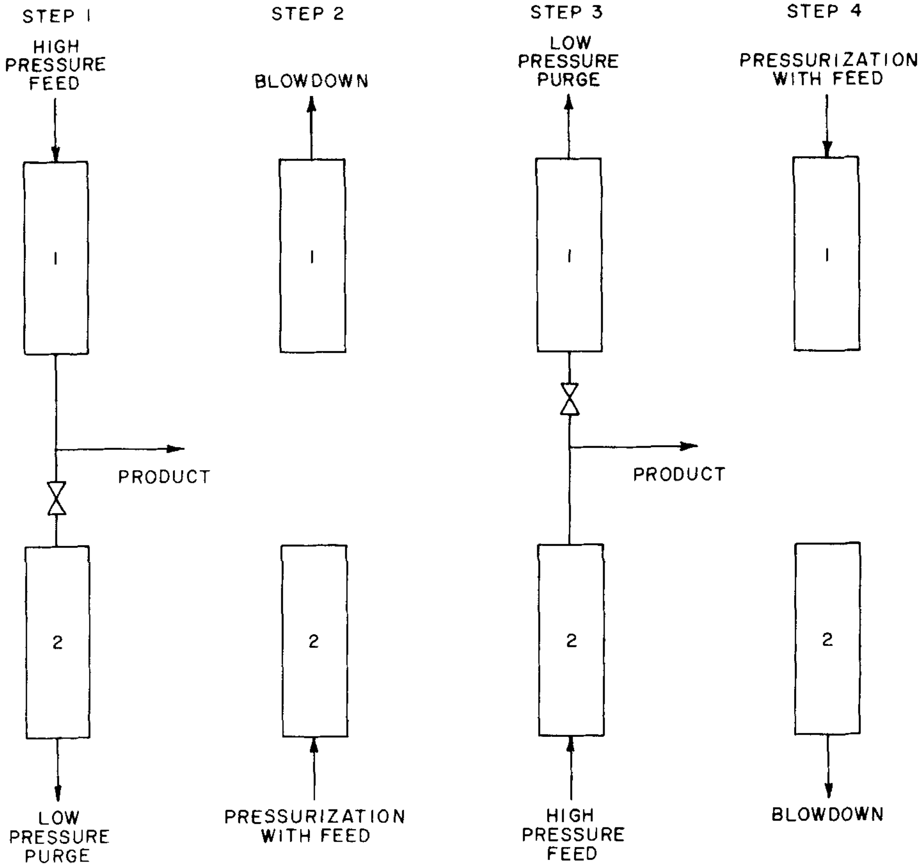

Figure 1. Steps in the pressure swing adsorption process.

Two modes of operation of this process were used. A so-called single-phase operating mode was realized when operating at 373 K and a two-phase mode at 298 K. Paths for these modes on the pressure-composition diagram for the vanadium-hydrogen system are shown in Figure 2. Pressure cycling between 103 kPa and 1030 kPa at 373 K resulted in operation wholly within the monohydride phase where the composition was $VH_{\sim 0.76}$. Operation between the same pressure limits at 298 K resulted in cycling between the monohydride and dihydride ($VH_{\sim 1.72}$) phases.

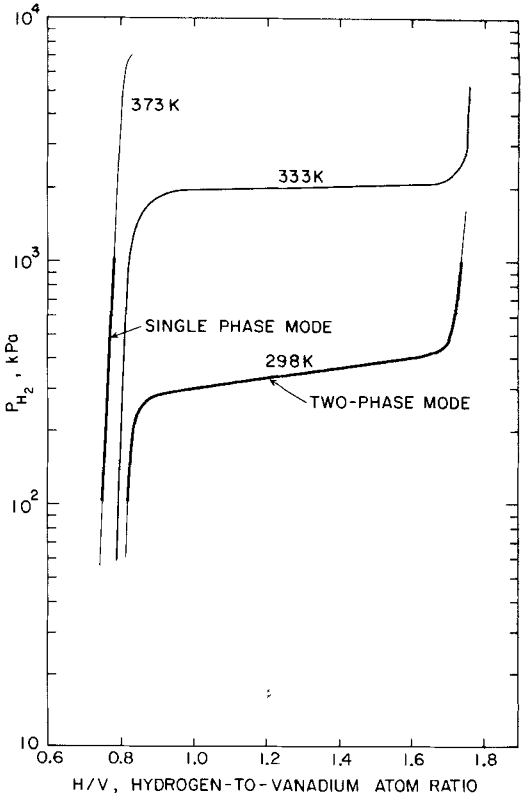

Figure 2. Operating modes of the pressure swing adsorption process. Pressure-composition data from Wong and Hill (14).

THEORY

Shendalman and Mitchell (16) presented an equilibrium theory of the separation of a two-component mixture via pressure swing adsorption. They treated the situation in which the cyclic operation is isothermal, one component is inert and is present in great excess, and the adsorption isotherm is linear. Chan et al. (17) extended the theory to the case in which both components are adsorbable, and the trace component is adsorbed preferentially. In both cases, development of the theory proceeded along the lines of the theory of parametric pumping (18), and the penetration distance concept (19) was used.

In this study, the treatment of Chan et al. (17) is applied to the removal of a trace quantity of HT from a stream of H_2 using vanadium hydride as the solid phase. For the sake of brevity, the theory will be presented for the separation conducted wholly in the monohydride phase.

The basic assumption in equilibrium theory is that the gas and solid phase are always at equilibrium with respect to the distribution of isotopic species. The applicable equilibrium relation is determined from the definition of the separation factor. For the exchange reaction of interest

$$HT(g) + H(VH_{0.7}) \rightleftarrows H_2(g) + T(VH_{0.7}) \tag{1}$$

the separation factor is defined as

$$\alpha = 2(C_{H_2}C_T)/(C_{HT}C_H) \tag{2}$$

This definition is valid when tritium is present at a trace level. As shown by Wong and Hill (14), α is a function of temperature but not of pressure.

By inspection of the pressure-composition diagram for the vanadium-hydrogen system (14), one sees that, in the monohydride phase, a pressure-composition isotherm within the pressure range of experimental interest may be approximated by

$$\ln p = aC_H + b \tag{3}$$

where a and b are functions of temperature.

Material balances for hydrogen and tritium over a differential length of a column are

$$\varepsilon\left[\frac{\partial C_{H_2}}{\partial t} + \frac{\partial (uC_{H_2})}{\partial z}\right] + (1-\varepsilon)\,\frac{1}{2}\,\frac{\partial C_H}{\partial t} = 0 \tag{4}$$

$$\varepsilon\left[\frac{\partial C_{HT}}{\partial t} + \frac{\partial (uC_{HT})}{\partial z}\right] + (1-\varepsilon)\,\frac{\partial C_T}{\partial t} = 0 \tag{5}$$

In these equations the gas flow is assumed to be one-dimensional, and axial dispersion is absent.

With the use of Equations (2) and (3) to eliminate C_T and C_H in Equations (4) and (5), and by assuming the perfect gas law and negligible pressure drop across a bed, the following equations may be obtained

$$\left[\frac{\varepsilon}{RT} + \frac{1-\varepsilon}{2ap}\right] \frac{\partial p}{\partial t} + \frac{\varepsilon P}{RT} \frac{\partial u}{\partial z} = 0 \tag{6}$$

and

$$\left[\frac{\varepsilon P}{RT} + (1-\varepsilon)\, \frac{\alpha}{2}\, C_H\right] \frac{\partial y}{\partial t} + \frac{\varepsilon u p}{RT} \frac{\partial y}{\partial z} + (1-\varepsilon)\, \frac{(\alpha-1)}{2}\, \frac{y}{ap}\, \frac{\partial p}{\partial t} = 0 \tag{7}$$

Following Chan et al. (17) and using the method of characteristics (20) to solve Equations (6) and (7), the following results can be obtained. During the constant pressure and purge steps, the position-versus-time characteristics are linear, and no changes in composition occur along them. Penetration distances for these steps are

$$L_H = u_H \Delta t / \left\{1 + [(1-\varepsilon)/\varepsilon]\, (RT/p_H)\, (\alpha/2) C_H(p_H)\right\} \tag{8}$$

$$L_L = u_L \Delta t / \left\{1 + [(1-\varepsilon)/\varepsilon]\, (RT/p_L)\, (\alpha/2) C_H(p_L)\right\} \tag{9}$$

For the pressurization and blowdown steps both the characteristic position changes and the composition changes along the characteristic:

$$z_H = J z_L \tag{10}$$

$$y_H = K y_L \tag{11}$$

where

$$J = \exp\left[-\int_{p_L}^{p_H} \frac{\varepsilon/(RT) + (1-\varepsilon)/(2ap)}{\varepsilon p/(RT) + (1-\varepsilon)(\alpha/2a)(\ln p-b)}\, dp\right] \tag{12}$$

$$K = \exp\left[-\int_{p_L}^{p_H} \frac{(1-\varepsilon)(\alpha-1)/(2ap)}{\varepsilon p/(RT) + (1-\varepsilon)(\alpha/2a)(\ln p-b)}\, dp\right] \tag{13}$$

Again following Chan et al., it can be shown that the critical purge-to-feed ratio is given by

$$G_{crit} = \frac{1}{J} \cdot \frac{p_L}{p_H} \cdot \frac{\varepsilon/(RT) + (1-\varepsilon)(\alpha/2)C_H(p_L)/p_L}{\varepsilon/(RT) + (1-\varepsilon)(\alpha/2)C_H(p_H)/p_H} \qquad (14)$$

When $G \geq G_{crit}$ and $L_H \leq h$, no HT will appear in the high pressure effluent at steady state; conversely, when $G < G_{crit}$ removal of HT will be incomplete.

The movement of characteristics for a case in which $G > G_{crit}$ is shown in Figure 3. For the example shown, the upper and lower columns are initially equilibrated with low and high pressure feed, respectively, and $L_L = 3L_H$, $z_H = 0.8z_L$ and $h = 10L_H$. The characteristics shown are those which divide the column into segments containing different mole fractions of HT. y_{av} denotes the average mole fraction within the column resulting from pressurization. The procedure for calculating this quantity is similar to that given by Chan et al. A general progression of tritium fronts toward the exhaust ends of the columns is seen. The product mole fraction for a given half cycle is equal to the product mole fraction for the previous half-cycle multiplied by the factor K, or

$$y_{n+1}^{PR} = Ky_n^{PR} \qquad n = 1,2,3,\ldots \qquad (15)$$

Initially $y_1^{PR} = Ky^F$. Hence

$$y_n^{PR} = K^n y^F \qquad (16)$$

and, since it turns out that $K<1$,

$$\lim_{n\to\infty} y_n^{PR} = 0 \qquad (17)$$

When operating with $G < G_{crit}$, HT does appear in the high pressure product stream at steady state. This situation is depicted in Figure 4 for the case in which $\frac{h-L_H}{J} < h$. For this case part of the HT introduced during the feed step is retained in the

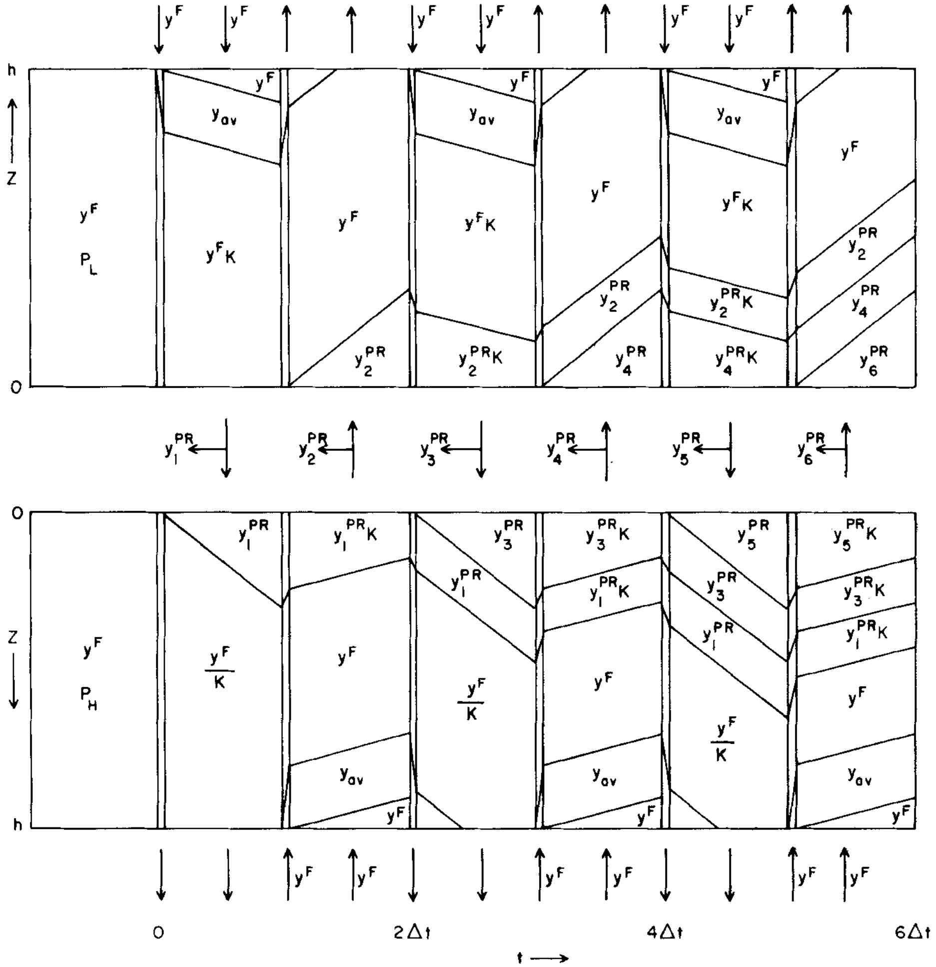

Figure 3. Illustration of the movement of characteristics for a case for which $G > G_{crit}$.

column after blowdown. In this figure the high pressure penetration distance is greater than that at the low pressure. In fact $L_H = 4\ L_L$ and $h = 10\ L_L$. The feed concentration eventually appears in the high pressure product stream.

In Figure 4, by geometry, $\frac{AB}{AC} = \frac{L_L J}{L_H}$ and $\frac{BC}{AC} = 1 - \frac{L_L J}{L_H}$. The mole fraction emerging from the column initially at high pressure is

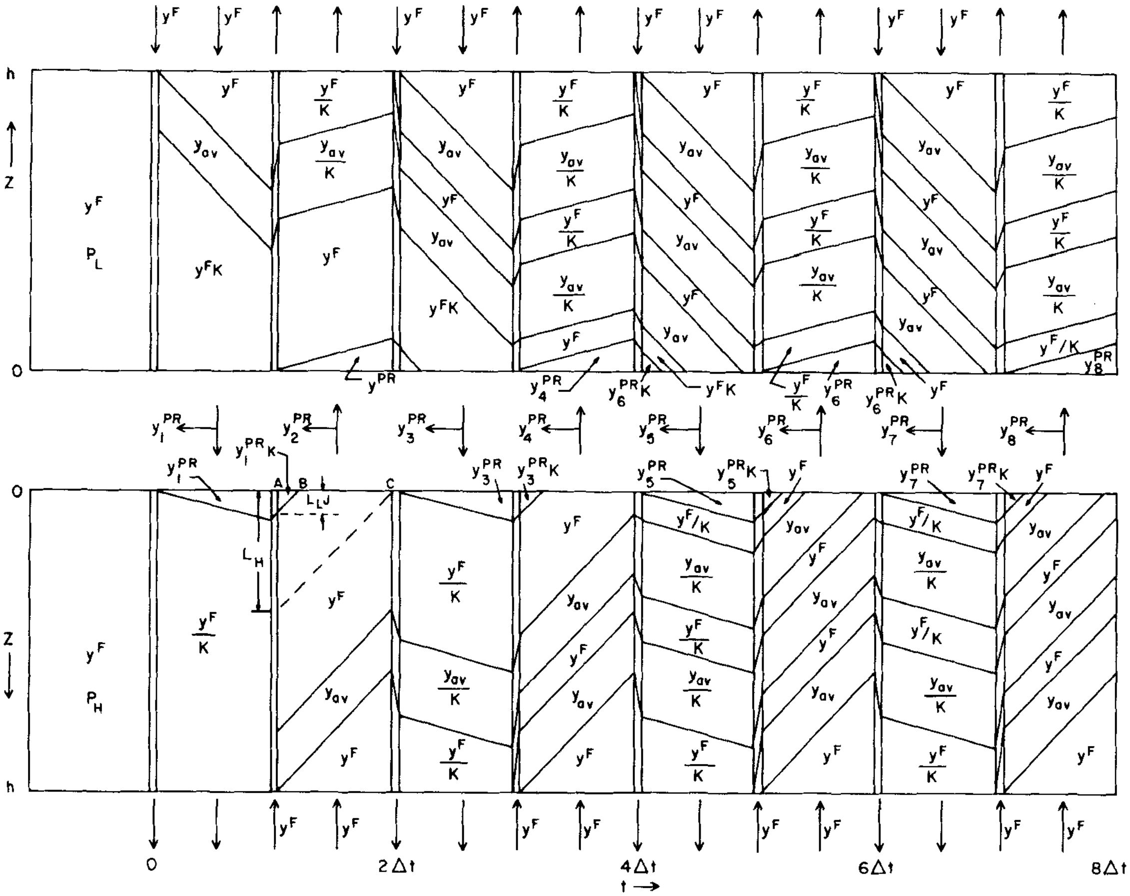

Figure 4. Illustration of the movement of characteristics for a case for which $G<G_{crit}$.

Ky_n^{PR}, n = 1,3,5,..., during the time interval AB and y^F during BC. Hence the average mole fraction is

$$y_{n+1}^{PR} = \frac{L_L J}{L_H} Ky_n^{PR} + (1 - \frac{L_L J}{L_H}) y^F, \quad n = 1,3,5,... \qquad (18)$$

The initial condition is $y_1^{PR} = Ky^F$. Similarly, the average HT mole fraction emerging from the column initially at low pressure is

$$y_{n+1}^{PR} = \frac{L_L J}{L_H} Ky_n^{PR} + (1 - \frac{L_L J}{L_H}) Ky^F, \quad n = 0,2,4,... \qquad (19)$$

The initial condition is $y_0^{PR} = y^F$.

Equations (18) and (19) can be used to calculate the average product mole fraction until the feed to the column initially at low pressure breaks through into the product stream. This occurs during the half cycle n = 2q + 1 where q is the smallest integer such that

$$(h-q\Delta L_L)J < L_H$$

After this half cycle, the high pressure effluent assumes a steady pattern which consists of concentration fronts derived from the feed and from the purge introduced to this column during the previous half cycle. For the situation depicted in Figure 4, the contribution from the feed can be further divided into two parts: the part derived from pressurization and that introduced during the constant pressure feed step. One sees that immediately after breakthrough of the feed introduced during the latter step, the high pressure product mole fraction is made up of four contributions whose weighted sum is

$$y_{2q+1}^{PR} = \frac{L_L J}{L_H} Ky_{2q}^{PR} + \frac{(h-q\Delta L_L)J - L_L J}{L_H} Ky^F$$

$$+ \frac{(h-q\Delta L_H) - (h-q\Delta L_L)J}{L_H} y_{av} + \frac{L_H - (h-q\Delta L_H)}{L_H} y^F \qquad (20)$$

After this half cycle, as can be seen from Figure 4, the average mole fraction from both columns can be described by Equation (20) except that the factor K is absent from the second term. It should be pointed out that Equation (20) is not a general expression for the breakthrough and mole fraction thereafter. Several other characteristic patterns are possible, and they are influenced by the penetration distances L_H and L_L.

For the case in which $\frac{h-L_H}{J} \geq h$, all the characteristics introduced during the feed step leave the column during blowdown. As a result, they will not appear in the product stream. The breakthrough mole fraction becomes

$$y_{2q+1}^{PR} = \frac{L_L J}{L_H} K y_{2q}^{PR} + \frac{(h-q\Delta L_L)J - L_L J}{L_H} K y^F + \frac{L_H-(h-q\Delta L_L)J}{L_H} y_{av} \tag{21}$$

and the mole fraction thereafter is

$$y_{n+1}^{PR} = \frac{L_L J}{L_H} K y_n^{PR} + \frac{\Delta L_H}{L_H} y_{av} \tag{22}$$

While analytical solution of Equations (18)-(22) or other similar equations is straightforward, it is just as convenient to evaluate them in stepwise fashion. The latter approach was taken in the present work. Constants required for numerical evaluation of the solutions were obtained from Wong and Hill (14).

Development of the theory for the two-phase operating mode follows exactly the same course as that given above except that the appropriate isotherm and separation factor must be used. As indicated in Figure 2, the isotherm at, say, 298 K is highly nonlinear. It was approximated for present purposes by a series of straight lines. The temperature dependence of the separation factor in the monohydride phase was measured by Wong and Hill (14) and in the dihydride phase by Wiswall and Reilly (13). Values from these sources were used for the extreme compositions of a two-phase experiment. Values at intermediate compositions were estimated by combining the extreme values according to the lever rule.

Rate processes of all kinds were ignored in the development of the above equilibrium theory. Therefore, when rate processes are important the theory should not be expected to agree well with the experiment. However the theory should provide bounding limits, valid when all rate processes are fast.

EXPERIMENTAL

Apparatus

A schematic diagram of the apparatus is shown in Figure 5. Each column was made of stainless steel, had an inside diameter of 0.77 x 10^{-2} m, and contained 0.06 kg of vanadium hydride particles. The packed bed had a void fraction of 0.5 and a length

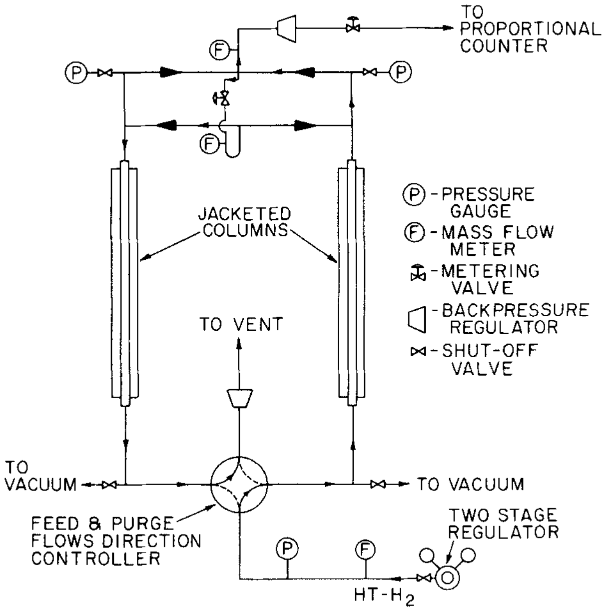

Figure 5. Schematic diagram of experimental apparatus.

of 45.7 x 10^{-2} m. The average particle size was 770 x 10^{-6} m (20-25 mesh). The bed was supported at the bottom by a stainless steel filter. Stainless steel wool was used to fill the space above the bed. The temperature of the column was maintained constant by means of a jacket and constant temperature circulating bath. Stainless steel sheathed chromel-alumel thermocouples 0.16 x 10^{-2} m in diameter were installed along the centerline of the columns with hot junctions located approximately 1.3 x 10^{-2} m from the product ends. The response time of these thermocouples was 1.2 s. Resistance heating wires wrapped around the outside of the jacket were used to raise the column temperature to levels as high as 720 K for the purpose of activating the vanadium particles. Hydrogen gas at high pressure was directed into the bottom of one column and purge gas at low pressure was introduced into the top of the other. This was achieved by a so-called feed and purge flow direction controller on the feed side and check valves on the product side. The flow direction controller consisted of an arrangement of four air-operated valves actuated by solid state timers. The valves were operated in such a way that one column was fed while the other was purged and vice versa.

As indicated in the Process Description section, the purge was derived from the high pressure column effluent. Thus part of the stream emerging from the high pressure column was withdrawn as product and the rest was let down to a lower pressure and introduced into the low pressure column as purge. The lowering of the pressure occurred as a result of the drop in pressure across a fine metering valve. The high pressure stream was prevented from direct entry into the low pressure column by a check valve. The pressure levels in the two columns were maintained by the feed gas regulator and the respective back pressure regulators. The column pressures and the pressure drops across the columns were measured by three high precision pressure gauges. The flow rates of the feed, the product and the purge were monitored by mass flow meters. All the valves used, except the fine metering valve, were bellow-sealed valves. A flow-through proportional counter of the kind described by Bernstein & Ballantine (21) was used to monitor the tritium level in the high pressure product stream. The gas flowing through the counter was a mixture of the product gas and P-10 counting gas. They were combined and mixed in a gas proportioner.

Materials

Hydrogen was obtained from the Matheson Gas Co., Rutherford, N. J., with a purity of 99.999%. Gaseous tritium was obtained from the New England Nuclear Corp., Boston, Mass., in the form of a one-curie ampoule, carrier free. A master batch of tritiated hydrogen was prepared by diluting the tritium with ~3 m^3 of the Matheson hydrogen. Feed for the experiments (~0.1 ppb mole fraction HT in H_2) was made up by dilution of 0.07 m^3 of the master batch with about 3 m^3 of the Matheson hydrogen. Ingots of vanadium were obtained from the Gallard-Schlesinger Chemical Manufacturing Corp., Carle Place, N. Y. The vanadium purity was 99.5% V minimum with major impurities in percent, 0.15 Si, 0.05 Fe, 0.04 N, 0.02 O, 0.03 C, 0.01 all other metals. Upon receipt the ingots were partially hydrided to facilitate crushing and sizing with standard sieves.

Procedure

The bed was activated in the following way. After charging the vanadium particles to the column, the bed was outgassed at 720 K until a vacuum better than 7×10^{-4} Pa was attained. The bed was then cooled to room temperature and pressurized with hydrogen to 1030 kPa. Hydrogen absorption was very rapid and was accompanied by rapid heat release. A bed temperature rise of 100 K was not unusual. After carrying out this procedure twice, the bed was considered to be fully activated. Prior to each pressure cycling run, one column was saturated with feed gas at high pressure p_H and the other was saturated with the same gas at low pressure p_L. This was achieved by feeding tritiated hydrogen gas at p_H to one column at a rate of 3.33×10^{-6} std m^3s^{-1} and allowing the emerging stream to bleed down to low pressure p_L and flow through the other column. The effluent of the latter column was monitored by the internal proportional counter until a steady state count rate was reached. The feed, product and purge flow rates were then adjusted to the conditions desired for the experimental run. The run was started by activating the solid state timers which controlled the switching of the air-operated valves. The count rate of tritium in the product stream was monitored until a steady state was achieved. Attainment of good reproducibility required reactivation of the beds after not more than four runs.

As indicated earlier the pressure cycling experiments were carried out in two different operating modes corresponding to cycling wholly within the monohydride phase and between this phase and the dihydride phase. The monohydride has a body-centered tetragonal lattice structure and the dihydride, a face-centered cubic structure. The structure remained constant with little change in hydrogen content during operation in the single phase mode but varied between the two structures with a large corresponding change in hydrogen content during two-phase mode operation. Absorption and desorption in the single phase mode were rapid processes whereas they were slow in the two-phase mode. As will be seen, differences in the rates of these processes in the two modes led to striking differences in their separation characteristics.

RESULTS AND DISCUSSION

Single-Phase Operating Mode

Experiments in this mode were conducted at 373 K with pressures varying in the range 103 to 1030 kPa (See Figure 2). The influence of each of the variables, G, Δt and p_H was determined.

Prior to conduct of the experiments or development of the theory it was anticipated that depletion of HT in the high pressure product would be predicted by an equilibrium theory and would be found experimentally. When the theory presented in this paper was used to calculate the HT steady state mole fraction to be expected in the high pressure product in the subcritical G-range ($G<G_{crit}$) for the single phase experiments, values negligibly less than the feed mole fraction were predicted. This turned out to be the case because the hydrogen content of the monohydride varied negligibly during cycling over the pressure ranges used. Also because of the small solid phase composition variation, G_{crit} was calculated to be very close to unity, so that complete removal of HT from the high pressure product could be expected only with no product withdrawal. Thus when considered to be a process taking place under conditions of equilibrium between gas and solid phases, it was predicted that no separation would be found over the entire G-range, and this prediction was independent of variation of Δt and p_H as well as G.

Instead of the depletion originally anticipated or the absence of separation predicted by theory, what was found experimentally was significant enrichment (Figures 6 to 8).

It is hypothesized that the cause of the enrichment was an isotope effect in the rates of absorption and desorption of hydrogen such that tritium is absorbed and desorbed more slowly than hydrogen. Support for this hypothesis and a discussion of some of the consequences of the kinetic isotope effect will be given prior to a detailed examination of the experimental results.

Absorption took place during the pressurization step and desorption during the blowdown step. Pressure changes occurred during these steps on a time scale of the order of 1 s or less in the experiments whereas the constant pressure steady flow rate feed and purge steps lasted for half cycle times ranging from 18 to 360 s. Wong and Hill (14) showed that the rate of tritium-

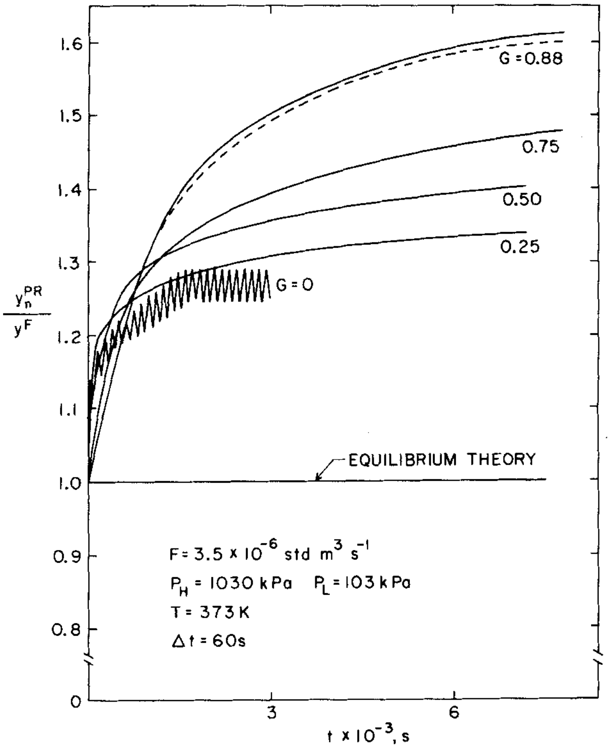

Figure 6. Dependence of high pressure product mole fraction transients on purge-to-feed ratio. Single-phase operating mode.

hydrogen exchange on vanadium monohydride occurring during the feed and purge steps was controlled by the surface exchange reaction, and they presented an Arrhenius type equation for the rate of exchange. From this equation one can calculate that the time scale for exchange at 373 K was approximately 90 s at 103 kPa and 20 s at 1030 kPa. These times are comparable to or shorter than most of the half-cycle times. It is therefore postulated that exchange during the feed and purge steps was usually at or near equilibrium. The observed enrichment then must be associated with the rapid pressure change steps.

Kinetic isotope effects are well known in exchange reactions involving hydrogen and its isotopes (22). Recent measurements of the rate of hydrogen absorption by tantalum (23) and by $LaCo_5$ and $LaNi_5$ alloys (24) showed that hydrogen was taken up more quickly than a heavier isotope, deuterium. If this were the case for hydrogen and tritium absorption by vanadium monohydride during pressurization and if hydrogen were desorbed more rapidly than tritium during blowdown, then tritium enrichment in the high pressure product would be expected. Slow tritium absorption relative to hydrogen absorption during pressurization would lead to tritium enrichment in the closed end of a column because of a higher effective migration velocity for tritium. Tritium would be further concentrated in the closed end of the column by a slower rate of desorption than that of hydrogen during blowdown. Then a lower effective migration velocity would lead to retention in the closed end. With the preceding discussion in mind, examination of the data and explanation of the effects observed can be undertaken.

The ratio of the high pressure product mole fraction of HT to the feed mole fraction is shown in Figure 6 as a function of time with the purge-to-feed ratio G as a parameter. For each value of G the ratio increases from unity corresponding to the feed mole fraction and ultimately approaches a steady state value significantly greater than unity. The transient for G=0 exhibits a cyclic oscillation which persists in the steady state. Such oscillations are not unexpected since the experiments are initiated after equilibration of one column at a high pressure and the other at a low pressure. The persistence of oscillations in the steady state may be due to a cyclic variation in product mole fraction similar to those implicit in Figure 4. A detailed model of the operation of the process when controlled by the kinetic isotope effect would be required to explain the oscillation quantitatively. Absence of the oscillations in the transients at higher values of G may be due at least in part to axial dispersion in the line to the counter. The flow rate in this line decreases as G increases. The reproducibility of these measurements is illustrated by the agreement of two runs for which G=0.88. Close agreement was facilitated by frequent, systematic reactivation of the hydride.

Enrichment of tritium in the high pressure product might be expected as a result of the presence of the kinetic isotope effect. Accumulation of tritium in a closed column end following pressurization results in appearance of a high HT mole fraction in the high pressure product in the course of the ensuing feed step. Amplification of this mole fraction in subsequent cycles results both from the introduction of HT into the product end of a column of purge gas bearing a high HT mole fraction and from accumulation in the same column end following blowdown as described earlier. Less amplification would result with a smaller purge rate and thus the steady state mole fraction would decrease as G decreases, as observed.

It should be mentioned that in early experiments in this study (15) no effect of G was perceived in the single phase mode. It is presently thought that this conclusion was drawn from experiments in which activation of the hydride particles was neither frequent enough nor systematic enough in procedure. No other significant differences were found between the later and earlier work in either operating mode.

Dimensionless high pressure product-to-feed mole fraction ratio transients are shown in Figure 7 with half-cycle time Δt as a parameter. The half-cycle time is proportional to L_H, the high pressure penetration distance. As one can see in Figure 7, the smaller L_H, the greater the product enrichment. This is an expected consequence of the kinetic isotope effect if the result of that effect is to produce a tritium mole fraction profile which decreases monotonically from the product end to the feed end of each column. Such a profile after pressurization is not unreasonable for a slowly absorbed trace component in a mixture with a rapidly absorbed major component.

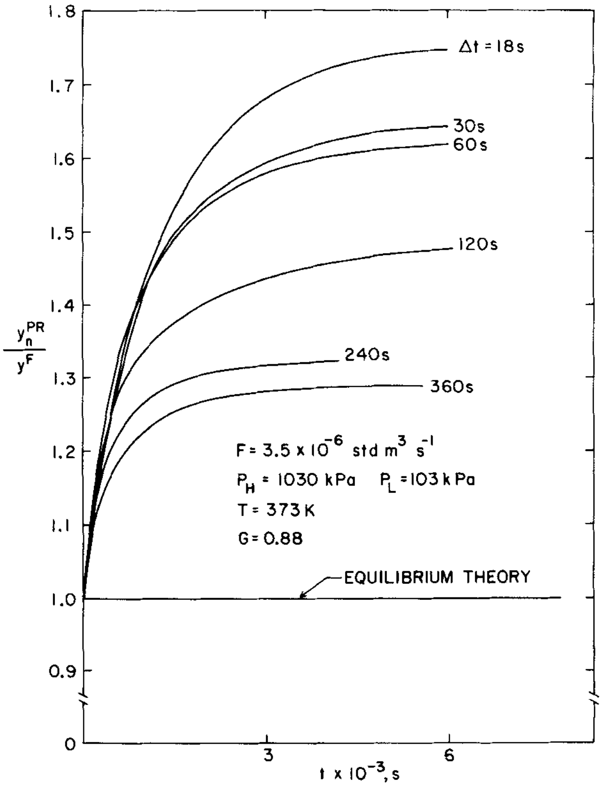

Figure 7. Dependence of high pressure product mole fraction transients on half-cycle time. Single-phase operating mode.

A further expected characteristic of the kinetic isotope effect is increase of the steady state product-to-feed mole fraction ratio with pressure ratio. This was found as shown in Figure 8. The pressure ratio was varied by varying P_H with P_L held constant at 103 kPa. The behavior observed is expected because increase of the pressure ratio would increase the concentration of tritium in the closed end of the column. Thus if a small pressure ratio were used a certain nonuniformity in mole fraction profile would result and a further increase in pressure would increase the nonuniformity.

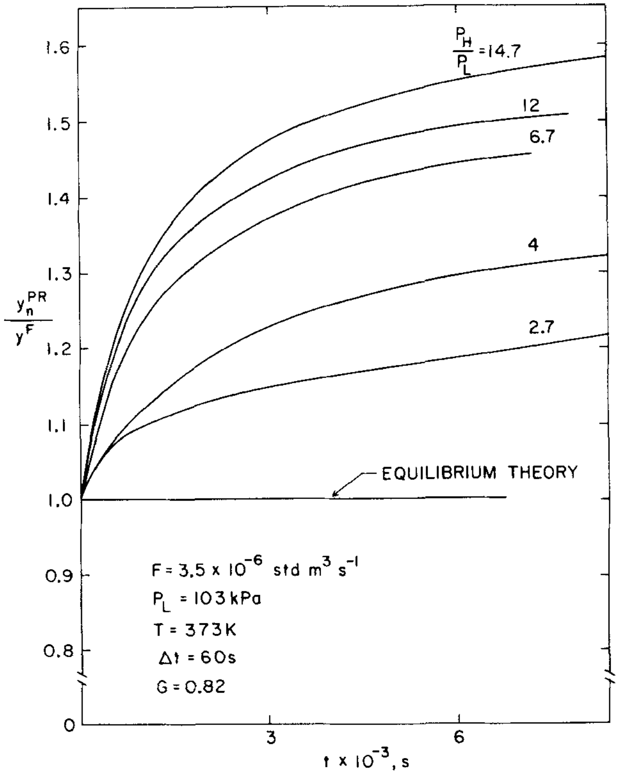

Figure 8. Dependence of high pressure product mole fraction transients on pressure ratio. Single-phase operating mode.

The variation of the steady state values of the dimensionless high pressure product HT mole fraction ratios with G, Δt and p_H seen in Figures 6 to 8 suggests that there are limiting values of these ratios as $G\to1$, $\Delta t\to0$, and $p_H/p_L\to\infty$. The existence of such limits was not systematically explored experimentally. It appears in principle however that control of these experiments by the kinetic isotope effect would lead to finite limits not much greater than those observed as $G\to1$ and $\Delta t\to0$ and a very large limiting ratio as p_H/p_L becomes large. In practice p_H/p_L could not be arbitrarily increased without encountering a phase transition.

Two Phase Operating Mode

Experiments in this mode were conducted at 298 K between the same pressure limits as those used in the single phase work (See Figure 2). The effects of the parameters Δt and G were examined. Depletion of HT in the high pressure product was predicted by equilibrium theory for these experiments and was found experimentally.

By using Equation (14) with J evaluated using the appropriate isotherm and separation factors for the two-phase experiments it was determined that $G_{crit}=0.55$.

Dimensionless product mole fraction transients with half-cycle time Δt as parameter are shown in Figure 9. In the experiments represented, G=0.88, well above the critical value. The shapes and steady state values of the transients for the four runs with Δt ranging from 600 to 4800 s are all very similar whereas the single transient with Δt = 300 s exhibits a rela-

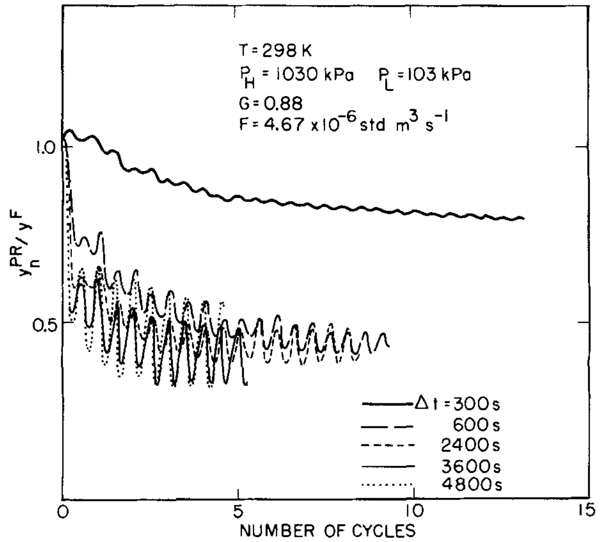

Figure 9. Dependence of high pressure product mole fraction transients on half-cycle time. Two-phase operating mode.

tively small oscillation and has a significantly higher steady state value. The reason for the difference in steady state values is apparent in Figure 10. This figure shows a few cycles of the temperature transients measured along a column centerline for three two-phase experiments with different values of Δt. Because of the large heat of dihydride formation (approximately 40 Kj/mole H_2) associated with the phase change, the constant temperature bath fluid circulating in the column jackets was not completely effective in maintaining the columns at a constant temperature of 298 K. (By contrast, in the single phase experiments where little change in hydride hydrogen content occurred, the column temperatures always stayed at 373 K.) Instead the column temperature rose above 298 K as the result of hydrogen absorption and heat release during the pressurization and feed steps and dropped below 298 K because of hydrogen desorption and heat absorption during the blowdown and purge steps. Return of the temperature to 298 K over about half of each half-cycle

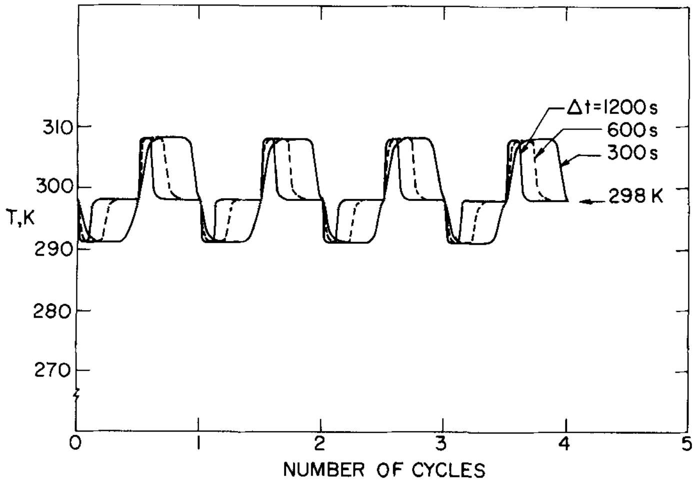

Figure 10. Steady state temperature transients measured for a few cycles along a column centerline. Two-phase operating mode.

occurred with a Δt of 600 s and over about three-quarters of each half-cycle with Δt = 1200 s. For these and longer half-cycles, during a significant portion of each half-cycle exchange took place as near equilibrium as possible in the two-phase mode. (Hysteresis is a known phenomenon in the two-phase region with absorption occurring at pressures 100 to 200 kPa higher than desorption. Thus the precise path or paths followed in these experiments is not known. Calculations using the theoretical expressions derived earlier but incorporating a hysteresis loop indicated a negligible difference in depletion from that corresponding to the 298 K path indicated in Figure 2.) For Δt = 300 s on the other hand neither absorption nor desorption was ever complete, for a plateau at 298 K was never observed as shown in Figure 10. Reasons for a high value of the steady state mole fraction ratio for the 300 s half-cycle time cannot be given unequivocally. The pressure-composition path or paths followed in the two columns are not known. Equilibrium was initially established in one column at low pressure when the solid was in the monohydride form. The starting material in the other column was the dihydride. All that can be said is that complete phase transitions evidently were never accomplished and that associated with this fact were observations of a higher steady state mole fraction ratio than those found when the phase transition was completed.

For experiments with longer half-cycle times, i.e., those which took place essentially at equilibrium, equilibrium theory would predict for super-critical purge-to-feed ratios no dependence of the steady state depletion on cycle time as long as breakthrough of feed into the high pressure product did not occur. The latter circumstance did not arise; the agreement of the steady state values is reasonably close, and these values show no systematic trend with Δt.

Failure to achieve complete removal of HT from the high pressure product will be discussed below in connection with the discussion of Figures 11 and 12.

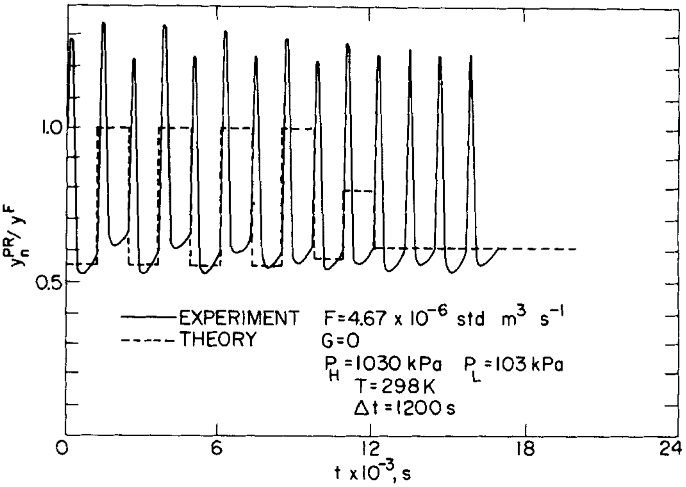

Figure 11. High pressure product mole fraction transient obtained with no purge (G=0). Two-phase operating mode.

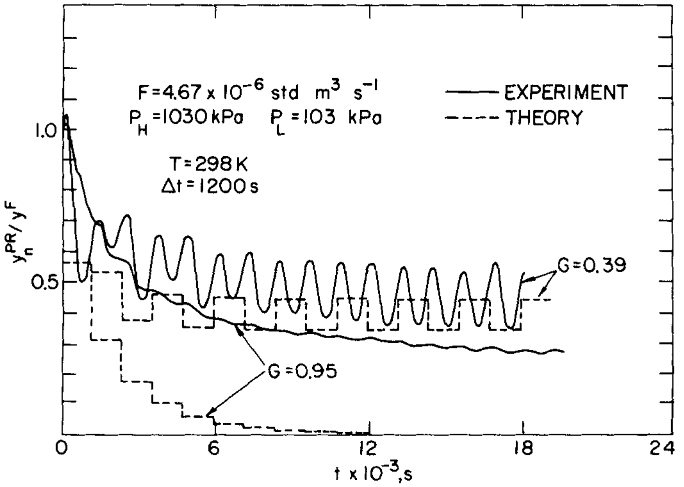

Figure 12. High pressure product mole fraction transients for G=0.38 and 0.95. G_{crit}=0.55. Two-phase operating mode.

Experimental dimensionless product-to-feed mole fraction ratio transients are shown in Figures 11 and 12 as a function of the purge-to-feed ratio G. The corresponding transients calculated from equilibrium theory are also shown. A half-cycle time of 1200 s was used to ensure that the phase transition was complete over a major portion of each half-cycle. In general HT depletion increased with G in agreement with equilibrium theory.

An interesting structure is seen in the detailed mole fraction ratio variation over each cycle. This structure changes with G. For G=0 (Figure 11), each odd half-cycle begins with a spike in the ratio which reaches a maximum value of roughly 1.25. This structure is compared in Figure 11 with the theoretical transient for the case for which $G<G_{crit}$ and $L_H<h$ (calculated using Equations (18)-(22)). In this transient for the first four cycles the value of the mole fraction ratio is 0.55 during each odd half-cycle and 1.0 during each even half-cycle. During the ninth half-cycle part of the feed breaks through into the high pressure product. This breakthrough continues thereafter and produces a steady state ratio value of 0.62. For the experiment in question the feed which breaks through is a portion of that introduced during the high pressure feed step. All of the latter and part of the former are expelled during blowdown. If the spikes were not present, the experimental and theoretical steady state ratios would be in good agreement, although, for unknown reasons, agreement is not good in the early even half-cycles.

The duration of the spikes was of the order of 300 to 400 s which is close to the time during which hydrogen was being absorbed as indicated by the temperature transients in Figure 10. The spikes, which have peak values well above the feed value, are considered to be further evidence of a kinetic isotope effect associated with hydrogen absorption. (In comparing the features of Figures 10 and 11 it should be remembered that the mole fraction transients are always those in the high pressure product as it emerges alternately from first one column and then the other. The temperature transients on the other hand are those found in a single column.)

Similar but diminished spikes were found in an experiment for which G=0.07 (not shown graphically). The spikes are missing from experiments at larger values of G (Figure 12). Their gradual disappearance is assumed to result from increasing axial dispersion in the product line leading to the in-line counter, as mentioned in connection with oscillations in the single phase experiments.

As mentioned earlier $G_{crit}=0.55$ for the two-phase experiments. Failure of the transients with higher purge-to-feed ratios - for the long Δt experiments in Figure 9 where G=0.88 and the experiment in Figure 12 with G=0.95 - to approach zero may have been due to two causes. First, the absorption and desorption processes occur on a time scale of some 300 to 400 s. These processes are thus far from being effectively instantaneous and are therefore responsible for mole fraction front broadening. Broadening would tend to prevent complete tritium removal. Second, introduction of tritium spikes with mole fractions which in the extreme might be in excess of the feed mole fraction into the product end of a column undergoing purging is counter to the ideal manner in which pressure swing processes are designed to work. Ideally purge gas is depleted of tritium rather than enriched in tritium. Both the finite rates of hydrogen uptake and release and the kinetic isotope effect would tend to prevent complete removal of tritium from the high pressure product.

Comparison of the Two Operating Modes

In Table 1 are listed values of the steady state high and low pressure product-to-feed mole fraction ratios and cuts (fractions of feed taken off as enriched product) with G as a parameter. The values of G and y_{∞}^{PR}/y^{F} were obtained experimentally. Values of y_{∞}^{BDPG}/y^{F} and the cut Θ were calculated from

TABLE 1

Steady State Stage Cuts and Separation Factors

Single phase mode: $F=3.5\times10^{-6}$ std m^3s^{-1}, $p_H=1030$ kPa, $p_L=103$ kPa
$T=373$ K, $\Delta t=60$ s

G	y_∞^{PR}/y^F	y_∞^{BDPG}/y^F	θ	α_s
0	1.27	0.87	0.32	1.46
0.25	1.34	0.89	0.24	1.50
0.5	1.41	0.92	0.16	1.54
0.75	1.48	0.97	0.08	1.53
0.88	1.64	0.98	0.04	1.68

Two phase mode: $F=4.67\times10^{-6}$ std m^3s^{-1}, $p_H=1030$ kPa, $p_L=103$ kPa

$T=298$ K, $\Delta t=1200$ s

G	y_∞^{PR}/y^F	y_∞^{BDPG}/y^F	Θ	α_s
0	0.62	1.19	0.66	1.92
0.39	0.44	1.14	0.79	2.59
0.95	0.29	1.01	0.98	3.48

tritium and hydrogen balances. Also listed is α_s, the effective stage separation factor, which is the enriched product mole fraction divided by the depleted product mole fraction. For both modes of operation, the stage separation factor increases with G but at the same time the cut approaches either zero (single-phase mode) or unity (two-phase mode). Cuts near 0.5 can be obtained but only with modest enrichment or depletion. If a multistage cascade were to be based on these modes of operation, it is conceivable that the two-phase process would be used in the enriching section, where cuts greater than 0.5 are desired, and the single-phase process would be used in the stripping section where cuts less than 0.5 are desired.

CONCLUSIONS

Process performance was controlled by one or the other of two isotope effects, depending on the mode of process operation. In the single phase mode, a postulated kinetic isotope effect appeared to control process performance. Experiments conducted with pressure cycling entirely in the monohydride phase resulted in enrichment of HT in the high pressure product stream rather than the absence of separation predicted by equilibrium theory. Enrichment was found to increase with purge-to-feed and pressure ratios and to decrease with half cycle time. It was possible to explain the observed behavior qualitatively in terms of a postulated isotope effect in the rates of hydrogen absorption and desorption.

In the two phase mode, process performance was mainly controlled by an equilibrium isotope effect. Experiments conducted with pressure cycling between the monohydride and dihydride phases resulted in depletion of HT in the high pressure product stream as expected with the equilibrium isotope effect of the vanadium-hydrogen system. Experiment and equilibrium theory were in good agreement at steady state at low purge-to-feed ratios although there was present evidence of the operation of the kinetic isotope effect. At purge-to-feed ratios greater than the critical value, HT removal from the high pressure product stream was incomplete, contrary to equilibrium expectations. This result was ascribed to concentration front broadening resulting from finite rates of hydrogen absorption and desorption during the phase transition, to tritium enrichment in the product end of the columns due to the kinetic isotope effect, and to axial diffusion.

ACKNOWLEDGEMENTS

This work was supported by the Division of Chemical Sciences, U. S. Department of Energy, Washington, D. C., under Contract #EY-76-C-02-0016.

NOTATION

a, b = empirical constants in Equation (3)
C_i = concentration of species i in the gas phase
$C_H(p_H)$, $C_H(p_L)$ = concentration of hydrogen atoms in hydride particles at high and low pressures, respectively
F = feed flow rate
G = purge-to-feed ratio
h = packed height of column
J = characteristic shift factor defined by Equation (12)
K = concentration change factor defined by Equation (13)
L = penetration distance of HT concentration front
ΔL_H = net displacement of a tritium front in a high pressure column after a complete cycle of operation, defined by $\Delta L_H = |L_L J - L_H|$
ΔL_L = net displacement of a tritium front in a low pressure column after a complete cycle of operation, defined by $\Delta L_L = |L_L - L_H \frac{1}{J}|$
n = half-cycle number
p = hydrogen pressure
q = smallest integer satisfying Equation (23)
R = gas constant
t = time
Δt = half-cycle time
T = temperature
u = interstitial gas velocity
y = mole fraction of HT in hydrogen stream
z = axial distance coordinate

Greek letters

α = tritium-protium separation factor
α_s = stage separation factor
Θ = stage cut, fraction of feed taken off as enriched product
ε = bed void fraction

Superscripts

BDPG = combined blowdown and purge
PR = high pressure product
F = feed

Subscripts

av = average
crit = critical
H = high pressure
L = low pressure
n = pertains to n^{th} half cycle

REFERENCES

1. E. Glueckauf and G. P. Kitt, Vapor Phase Chromatography, Butterworths Scientific Publications, (D. E. Desty, ed.), London, 1957, p. 422.

2. H. A. Smith and E. H. Carter, in Tritium in the Physical and Biological Sciences, Vol. 1, International Atomic Energy Agency, Vienna, 1962, p. 121.

3. A. Zlatkis and V. Pretorius, Preparative Gas Chromatography, Wiley-Interscience, New York, 1971.

4. C. W. Skarstrom, Annals of N. Y. Acad. of Sci., 72, 750, 1959.

5. J. K. Wagner and H. A. Stewart, Paper presented at the 3rd Joint I.I.Q.P.R.-A.I.Ch.E. Meeting, San Juan, Puerto Rico, May 1970.

6. P. E. Barker, in Progress in Separation and Purification, Vol. 4, (E. S. Perry and J. Van Oss, eds.), Wiley-Interscience, New York, 1971.

7. R. Pigford, B. Barker III and D. E. Blum, Ind. Engng. Chem. Fundl., 8, 848, 1969.

8. P. C. Wankat, Ind. Engng. Chem. Fundl., 14, 96, 1975.

9. R. H. Wilhelm, A. W. Rice and A. R. Bendelius, Ind. Engng. Chem. Fundl., 5, 141, 1966.

10. J. D. Stokes and H. T. Chen, Ind. Engng. Chem. Process Des. Dev., 18, 147, 1979.

11. K. Weaver and C. E. Hamrin, Jr., Chem. Eng. Sci., 29, 1973, 1974.

12. J. J. Reilly and R. H. Wiswall, Jr., Inorg. Chem., 9, 1678, 1970.

13. R. H. Wiswall, Jr. and J. J. Reilly, Inorg. Chem., 11, 1691, 1972.

14. Y. W. Wong and F. B. Hill, AIChE J., 25, 592, 1979.

15. F. B. Hill, Y. W. Wong and Y. N. I. Chan, Proc. 15th DOE Air Cleaning Conf., (M. W. First, Ed.), Vol. 1, 1978, p. 167.

16. L. H. Shendalman and J. E. Michell, Chem. Eng. Sci., 27, 1449, 1972.

17. Y. N. I. Chan, F. B. Hill and Y. W. Wong, submitted to Chem. Eng. Sci.

18. R. L. Pigford, B. Baker III and D. E. Blum, Ind. Engng. Chem. Fundl., 8, 144, 1969.

19. H. T. Chen and F. B. Hill, Separation Sci., 6, 411, 1971.

20. R. Aris and N. R. Amundson, Mathematical Methods in Chemical Engineering, Vol. 2, Prentice Hall, 1973.

21. W. Bernstein and R. Ballentine, Rev. Sci. Instr., 21, 158, 1950.

22. L. Melander, Isotope Effects on Reaction Rates, The Ronald Press Company, New York, 1960.

23. J. M. Guil, D. O. Hayward and N. Taylor, Proc. Roy. Soc. Lond. A., 335, 141, 1973.